

The SOPHIE search for northern extrasolar planets[★]

II. A multiple planet system around HD 9446

G. Hébrard¹, X. Bonfils², D. Ségransan³, C. Moutou⁴, X. Delfosse², F. Bouchy^{1,5}, I. Boisse¹, L. Arnold⁵, M. Desort², R. F. Díaz¹, A. Eggenberger², D. Ehrenreich², T. Forveille², A.-M. Lagrange², C. Lovis³, F. Pepe³, C. Perrier², F. Pont⁶, D. Queloz³, N. C. Santos^{3,7}, S. Udry³, and A. Vidal-Madjar¹

¹ Institut d'Astrophysique de Paris, UMR7095 CNRS, Université Pierre & Marie Curie, 98bis boulevard Arago, 75014 Paris, France
e-mail: hebrard@iap.fr

² Université J. Fourier (Grenoble 1)/CNRS, Laboratoire d'Astrophysique de Grenoble (LAOG, UMR5571), France

³ Observatoire de Genève, Université de Genève, 51 Chemin des Maillettes, 1290 Sauverny, Switzerland

⁴ Laboratoire d'Astrophysique de Marseille, Université de Provence, CNRS (UMR 6110), BP 8, 13376 Marseille Cedex 12, France

⁵ Observatoire de Haute-Provence, CNRS/OAMP, 04870 Saint-Michel-l'Observatoire, France

⁶ School of Physics, University of Exeter, Exeter, EX4 4QL, UK

⁷ Centro de Astrofísica, Universidade do Porto, Rua das Estrelas, 4150-762 Porto, Portugal

Received 2 December 2009 / Accepted 5 January 2010

ABSTRACT

We report the discovery of a planetary system around HD 9446, performed from radial velocity measurements secured with the spectrograph *SOPHIE* at the 193-cm telescope of the Haute-Provence Observatory for more than two years. At least two planets orbit this G5V, active star: HD 9446b has a minimum mass of $0.7 M_{\text{Jup}}$ and a slightly eccentric orbit with a period of 30 days, whereas HD 9446c has a minimum mass of $1.8 M_{\text{Jup}}$ and a circular orbit with a period of 193 days. As for most of the known multiple planet systems, the HD 9446-system presents a hierarchical disposition with a massive outer planet and a lighter inner planet.

Key words. planetary systems – techniques: radial velocities – stars: individual: HD 9446

1. Introduction

Among the more than 400 exoplanets known so far, most of them have been discovered from the reflex motion they cause to their host-star, which can be detected from stellar radial velocity wobble. Thus, accurate radial velocity measurements remain a particularly efficient and powerful technique for research and characterization of exoplanetary systems. They allow the statistics of systems to be extended by completing the minimum mass-period diagram of exoplanets, in particular towards lower masses and longer periods, as the measurement accuracy improves.

Together with the advent of the new *SOPHIE* spectrograph at the 1.93-m telescope of Haute-Provence Observatory (OHP), France, the *SOPHIE* Consortium (Bouchy et al. 2009) started a large observational program in late 2006 of exoplanet search and characterization, using the radial velocity technique. In the present paper we announce the discovery of two exoplanets around HD 9446, from radial velocity measurements secured as part of the second sub-program of the *SOPHIE* Consortium. This sub-program is a giant-planet survey on a volume-limited sample around 2000 FGK stars, requiring moderate accuracy, typically in the range $5\text{--}10\text{ m s}^{-1}$ (Bouchy et al. 2009). Its goal is

to improve the statistics on the exoplanet parameters and their hosting stars by increasing the number of known Jupiter-mass planets, as well as to offer a chance to find new transiting giant planets in front of bright stars. *SOPHIE* sub-program-2 data have already been used to report detection of several planets (Da Silva et al. 2008; Santos et al. 2008; Bouchy et al. 2009) and to study stellar activity (Boisse et al. 2009a). This sub-program also aims at following up transiting giant exoplanets. This allowed spectroscopic transits to be observed (Loeillet et al. 2008), including the detection of the two first cases of spin-orbit misalignment, namely XO-3b (Hébrard et al. 2008) then HD 80606b (Moutou et al. 2009; Pont et al. 2009), simultaneously with the discovery of the transiting nature of the planet in this last case.

The *SOPHIE* observations of HD 9446 that allowed detection of two new planets are presented in Sect. 2. We derive and discuss the stellar and planetary properties in Sects. 3 and 4, respectively, and conclude in Sect. 5.

2. Observations

We observed HD 9446 with the OHP 1.93-m telescope and *SOPHIE*, which is a cross-dispersed, environmentally stabilized echelle spectrograph dedicated to high-precision radial velocity measurements (Perruchot et al. 2008; Bouchy et al. 2009). Observations were secured in *high-resolution* mode, allowing the resolution power $\lambda/\Delta\lambda = 75\,000$ to be reached. The spectra were obtained in three seasons, from November 2006 to March 2009. Depending on variable atmospheric conditions, the exposure times ranged between 3 and 18 min, and the

[★] Based on observations collected with the *SOPHIE* spectrograph on the 1.93-m telescope at Observatoire de Haute-Provence (CNRS), France, by the *SOPHIE* Consortium (program 07A.PNP.CONNS). The full version of Table 1 (*SOPHIE* measurements of HD 9446) is only available in electronic form at the CDS via anonymous ftp to cdsarc.u-strasbg.fr (130.79.128.5) or via <http://cdsweb.u-strasbg.fr/cgi-bin/qcat?J/A+A/513/A69>

Table 1. Radial velocities of HD 9446 measured with *SOPHIE* (full table available at the CDS).

BJD	RV	$\pm 1\sigma$
-2 400 000	(km s ⁻¹)	(km s ⁻¹)
54 043.4849	21.7152	0.0063
54 045.4850	21.7451	0.0055
54 047.4598	21.7747	0.0056
54 048.5033	21.7969	0.0054
...
...
54 889.2599	21.7201	0.0073
54 890.2628	21.7409	0.0064
54 893.2986	21.7222	0.0090
54 894.2961	21.7074	0.0097

signal-to-noise ratios per pixel at 550 nm were between 32 and 94, with typical values of 5.5 min and 55, respectively. Exposure time and signal-to-noise ratio were slightly greater during the first season of observation. Three exposures performed under too cloudy conditions were excluded from the final dataset, which includes 79 spectra. The total exposure time is about 7 h.

The spectrograph is fed by two optical fibers, the first one used for starlight. During the first season, the second *SOPHIE* entrance fiber was fed by a thorium lamp for simultaneous wavelength calibration. Thereafter we estimated that wavelength calibration performed with a ~ 2 -h frequency each night (allowing interpolation for the time of the exposure) was sufficient and that the instrument was stable enough to avoid simultaneous calibration for this moderately accurate program. For the second and third seasons, therefore, no simultaneous thorium calibration were performed, avoiding pollution of the first-entrance spectrum by the calibration light. The second entrance fiber was instead put on the sky, and this allowed us to check that none of the spectra were significantly affected by sky background pollution, especially from moonlight.

We used the *SOPHIE* pipeline (Bouchy et al. 2009) to extract the spectra from the detector images, cross-correlate them with a G2-type numerical mask, then fit the cross-correlation functions (CCFs) by Gaussians to get the radial velocities (Baranne et al. 1996; Pepe et al. 2002). Each spectrum produces a clear CCF, with a 8.47 ± 0.05 km s⁻¹ full width at half maximum and a contrast representing $38.0 \pm 0.8\%$ of the continuum. Only the 33 first spectral orders of the 39 available ones were used for the cross correlation. This allows the full dataset to be reduced with the same procedure, because the last red orders of the HD 9446 spectra obtained during the first season were polluted by argon spectral lines of the simultaneous wavelength calibration.

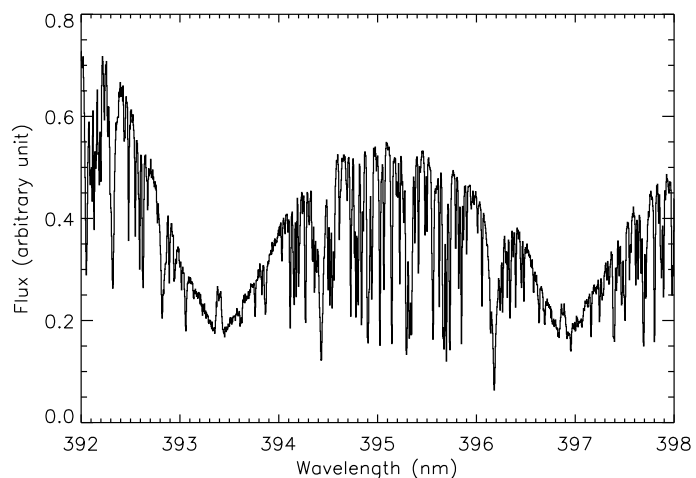
The derived radial velocities are reported in Table 1. The accuracies are between 5.4 and 9.7 m s⁻¹, typically around 6.5 m s⁻¹. This includes photon noise (typically ~ 3.5 m s⁻¹), wavelength calibration (~ 2 m s⁻¹), and guiding errors (~ 5 m s⁻¹) that produce motions of the input image within the fiber (Boisse et al. 2009b). These computed uncertainties do not include any “jitter” due to stellar activity (see below).

3. Stellar properties of HD 9446

We used the 50 *SOPHIE* spectra secured without simultaneous thorium exposure to obtain an averaged spectrum, and we managed to do a spectral analysis from it. Table 2 summarizes the stellar parameters. According to the SIMBAD database, HD 9446 (HIP 7245, BD+28 253) is a $V = 8.35$, high

Table 2. Adopted stellar parameters for HD 9446.

Parameters	Values
m_b	8.35
Spectral type	G5V
$B - V$	0.680 ± 0.015
Parallax [mas]	19.92 ± 1.06
Distance [pc]	53 ± 3
$v \sin i_*$ [km s ⁻¹]	4 ± 1
$\log R'_{\text{HK}}$	-4.5 ± 0.1
[Fe/H]	0.09 ± 0.05
T_{eff} [K]	5793 ± 22
$\log g$ [cgs]	4.53 ± 0.16
Mass [M_{\odot}]	1.0 ± 0.1
Radius [R_{\odot}]	1.0
Luminosity [L_{\odot}]	1.1

**Fig. 1.** H and K Ca II lines of HD 9446 on the averaged *SOPHIE* spectra. Chromospheric emissions are detected, yielding a $\log R'_{\text{HK}} = -4.5 \pm 0.1$.

proper-motion G5V star. Its Hipparcos parallax ($\pi = 19.92 \pm 1.06$ mas) implies a distance of 53 ± 3 pc. The Hipparcos color is $B - V = 0.680 \pm 0.015$ (Perryman et al. 1997).

From spectral analysis of the *SOPHIE* data using the method presented in Santos et al. (2004), we derived the temperature $T_{\text{eff}} = 5793 \pm 22$ K, the gravity $\log g = 4.53 \pm 0.16$, $[\text{Fe}/\text{H}] = +0.09 \pm 0.05$, and $M_* = 1.0 \pm 0.1 M_{\odot}$. The 10% uncertainty on the stellar mass is an estimation, because systematic effects are difficult to quantify (Fernandes & Santos 2004). We derived a projected rotational velocity $v \sin i_* = 4 \pm 1$ km s⁻¹ from the parameters of the CCF using the calibration of Boisse et al. (in preparation), which is similar to that presented by Santos et al. (2002). We also obtained $[\text{Fe}/\text{H}] = +0.12 \pm 0.10$ from the CCF, which agrees with, but is less accurate than, the metallicity obtained from our spectral analysis.

The cores of the large Ca II absorption lines of HD 9446 show weak emission (Fig. 1), which is the signature of an active chromosphere. Such stellar activity would imply a significant “jitter” on the stellar radial velocity measurement. The level of the Ca II emission corresponds to $\log R'_{\text{HK}} = -4.5$ with a ± 0.1 dispersion according to the *SOPHIE* calibration (Boisse et al. in preparation). For a G-type star with this level of activity, Santos et al. (2000) predict a dispersion of 10 to 20 m s⁻¹ for the stellar jitter. According to Noyes et al. (1984) and Mamajek & Hillenbrand (2008), this level of activity implies a stellar rotation period $P_{\text{rot}} \approx 10$ days. This agrees with our $v \sin i_*$ measurement, which translates into $P_{\text{rot}} < 17$ days (Bouchy et al. 2005),

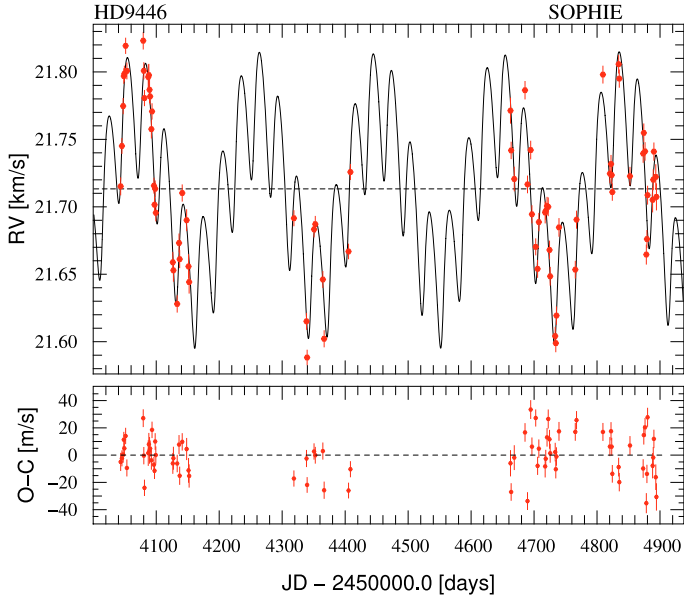


Fig. 2. *Top:* radial velocity *SOPHIE* measurements of HD 9446 as a function of time, and Keplerian fit with two planets. The orbital parameters corresponding to this fit are reported in Table 3. *Bottom:* residuals of the fit with $1\text{-}\sigma$ error bars.

depending on the unknown inclination i_\star of the stellar rotation axes.

4. A planetary system around HD 9446

The *SOPHIE* radial velocities of HD 9446 are plotted in Fig. 2. Spanning more than two years, they show clear variations of about 200 m s^{-1} , implying a dispersion $\sigma_{\text{RV}} = 58 \text{ m s}^{-1}$. This is well over the expected stellar jitter due to chromospheric activity (10 to 20 m s^{-1} , see above). In addition, the bisectors of the CCF are stable (Fig. 3, upper panel), showing dispersion of $\sigma_{\text{BIS}} \approx 20 \text{ m s}^{-1}$, well below that of the radial velocities. An anticorrelation between the bisector and the radial velocity is usually the signature of radial velocity variations induced by stellar activity (see, e.g., Queloz et al. 2001; Boisse et al. 2009a). The bisectors are flat by comparison with the radial velocities, which suggests that the radial velocity variations mainly stem from Doppler shifts of the stellar lines rather than stellar profile variations. This leads to concluding that reflex motion due to companion(s) is the likely cause of the stellar radial velocity variations.

These facts were known in late 2007, after two seasons of *SOPHIE* observations of HD 9446. A search of Keplerian fits then produced a solution with two Jupiter-like planets, on orbits of 30 and 190-day periods, with low eccentricities. This solution was thereafter confirmed by the third season of observation. Together with the “flat” bisectors, this provides strong support for the two-planet interpretation of the radial velocity variations.

Figures 2 and 4 show the final fit of the 851-day span *SOPHIE* radial velocities of HD 9446. This Keplerian model includes two planets without mutual interactions, which are negligible in this case (see Sect. 5). All the parameters are free to vary during the fit. The derived orbital parameters are reported in Table 3, together with error bars, which were computed from χ^2 variations and Monte Carlo experiments.

The inner planet, HD 9446b, produces radial velocity variations with a semi-amplitude $K = 46.6 \pm 3.0 \text{ m s}^{-1}$, corresponding

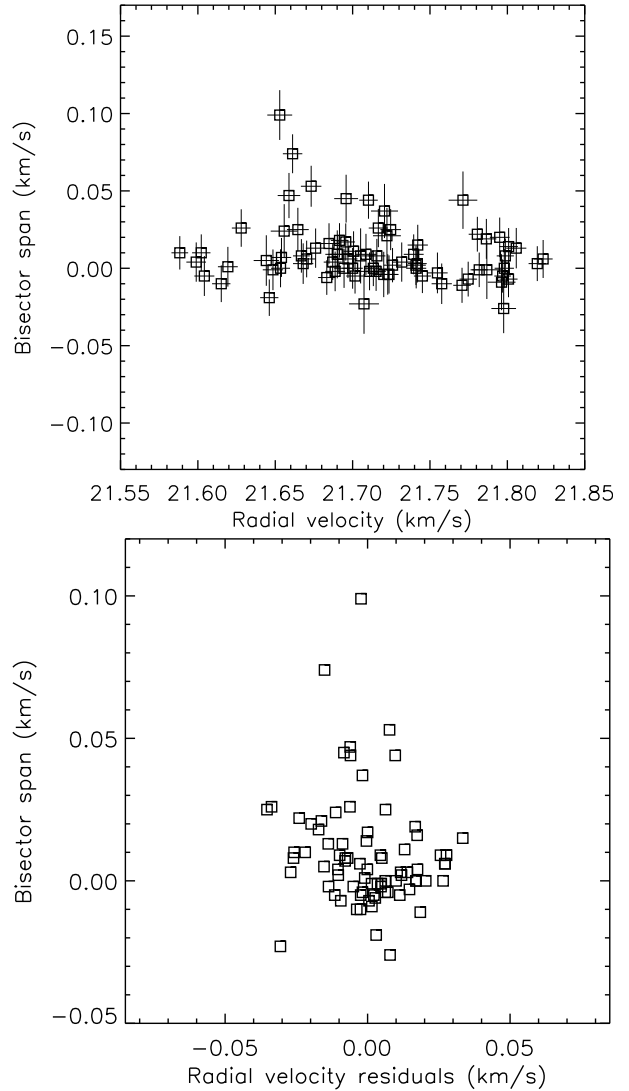


Fig. 3. Bisector span as a function of the radial velocity (*top*) and the radial velocity residuals after the 2-planet fit (*bottom*). For clarity, error bars are not plotted in the *bottom* panel. The ranges have the same extents as in the x - and y -axes on both panels.

to a planet with a minimum mass $M_p \sin i = 0.70 \pm 0.06 M_{\text{Jup}}$ (assuming $M_\star = 1.0 \pm 0.1 M_\odot$ for the host star). Its orbit has a period of 30.052 ± 0.027 days, and is significantly non circular ($e = 0.20 \pm 0.06$). This period is longer than the stellar rotation period, as determined above from the $\log R'_{\text{HK}}$ and the $v \sin i_\star$. A P_{rot} -value of 30 days would correspond to $v \sin i_\star < 2 \text{ km s}^{-1}$, which is incompatible with our data. The outer planet, HD 9446c, yields a semi-amplitude $K = 63.9 \pm 4.3 \text{ m s}^{-1}$, corresponding to a planet with a projected mass $M_p \sin i = 1.82 \pm 0.17 M_{\text{Jup}}$. The orbital period is 192.9 ± 0.9 days. This is about half an Earth year, which made a good phase coverage difficult for the observations. As seen in the lower panel of Fig. 4, the rise of the radial velocity due to HD 9446c lacks measurements for orbital phases between 0.0 and 0.3. This implies significant uncertainties on the shape of the orbit. Circularity cannot be excluded ($e = 0.06 \pm 0.06$); furthermore, if the orbit actually is eccentric, there are hardly no constraints with the present dataset on the orientation of the ellipse with respect to the line of sight. The resulting error bars on the longitude ω of the periastron and on the time T_0 at periastron are thus large; they however, are

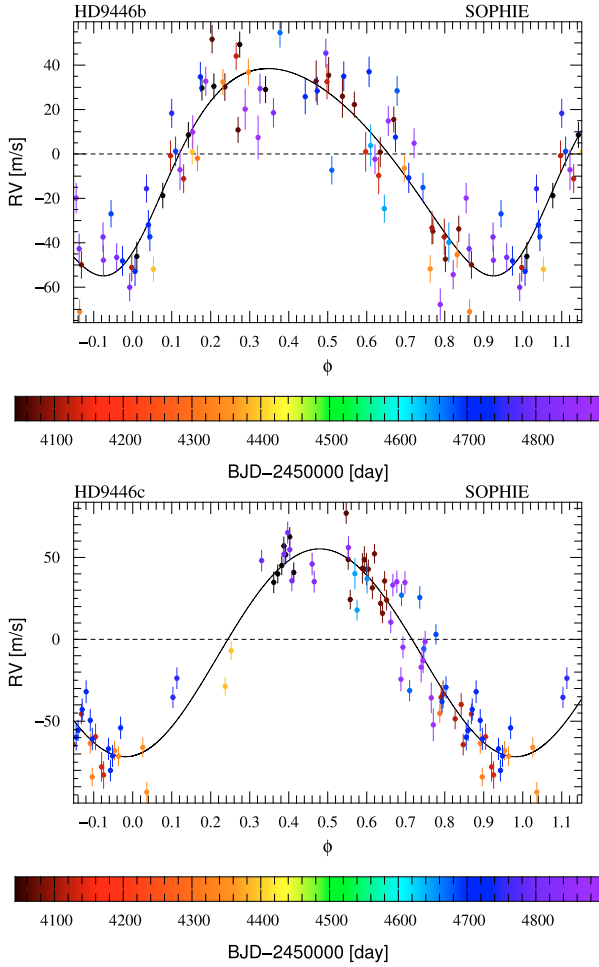


Fig. 4. Phase-folded radial velocity curves for HD 9446b ($P = 30$ d, *top*) and HD 9446c ($P = 193$ d, *bottom*) after removing the effect of the other planet. The *SOPHIE* radial velocity measurements are presented with $1\text{-}\sigma$ error bars, and the Keplerian fits are the solid lines. Orbital parameters corresponding to the fits are reported in Table 3. The colors indicate the measurement dates.

correlated, and the timing of a possible transit for this planet is better constrained than T_0 in Table 3. Our estimations of $v \sin i_*$ and P_{rot} allow the constraint $i_* > 30^\circ$ to be put, so if we assume a spin-orbit alignment for the HD 9446-system, $i_* = i$ and $\sin i > 0.5$, and this implies projected masses that translate into actual masses clearly in the planetary range.

The reduced χ^2 of the Keplerian fit is 2.6, and the standard deviation of the residuals is $\sigma_{\text{O-C}} = 15.1 \text{ m s}^{-1}$. This is better than the 58-m s^{-1} dispersion of the original radial velocities, but this remains higher than the 6.5-m s^{-1} typical error bars on the individual measurements, suggesting an additional noise of $\sim 13.5 \text{ m s}^{-1}$. Such a dispersion is precisely in the range of the 10 to 20 m s^{-1} expected jitter for a G-type star with this level of activity (Sect. 3). Stellar activity is thus likely to be the main cause of the remaining dispersion, as well as the $\sim 20\text{-m s}^{-1}$ dispersion of the bisectors. The residuals of the fits do not show any significant anticorrelation with the bisectors (Fig. 3, lower panel), as it could be expected in such cases (see, e.g., Melo et al. 2007; Boisse et al. 2009a). This is however at the limit of detection according to the error bars. A few bisectors values are larger than the other ones. They could come from a particularly active phase of the star, as they are localized in a short time interval (between late January and early February 2007). Excluding

Table 3. Fitted orbits and planetary parameters for the HD 9446 system, with $1\text{-}\sigma$ error bars.

Parameters	HD 9446b	HD 9446c
P [days]	30.052 ± 0.027	192.9 ± 0.9
e	0.20 ± 0.06	0.06 ± 0.06
ω [$^\circ$]	-145 ± 30	-260 ± 130
K [m s^{-1}]	46.6 ± 3.0	63.9 ± 4.3
T_0 (periastron) [BJD]	$2\,454\,854.4 \pm 2.0$	$2\,454\,510 \pm 70$
$M_{\text{p}} \sin i$ [M_{Jup}]	$0.70 \pm 0.06^\dagger$	$1.82 \pm 0.17^\dagger$
a [AU]	$0.189 \pm 0.006^\dagger$	$0.654 \pm 0.022^\dagger$
V_r [km s^{-1}]	21.715 ± 0.005	
N	79	
reduced χ^2	2.6	
$\sigma_{\text{O-C}}$ [m s^{-1}]	15.1	
Typical RV accuracy [m s^{-1}]	6.5	
span [days]	851	

Notes. † : using $M_* = 1.0 \pm 0.1 M_\odot$.

these outliers from the analysis does not significantly change the results. Finally, as seen in the lower panel of Fig. 2, the residuals are significantly less scattered during the first season than during the third one. This can be explained mainly by the higher signal-to-noise ratio reached with longer exposure times during the first season, as well as the simultaneous thorium calibration secured for the first measurements.

Figure 5 shows Lomb-Scargle periodograms of the radial velocity measurements of HD 9446 in four different cases: without any planet removed, with one or the other planet removed, and with both planets removed. A similar study was performed in the case of BD $-08^\circ 2823$, another star with two detected planets (Hébrard et al. 2009). In the upper panel of Fig. 5 that presents the periodogram of the raw radial velocity measurements of HD 9446, periodic signals at ~ 30 days and ~ 195 days are clearly detected with peaks at those periods, corresponding to the two planets reported above, with the same amplitudes. The peak at ~ 1 day corresponds to the aliases of all the detected signals, as the sampling is biased towards “one point per night”. A fourth, weaker peak is detected at ~ 13.3 days. A Keplerian fit of this signal would provide a semi-amplitude $K \approx 11 \text{ m s}^{-1}$, corresponding to a projected mass of 40 Earth masses. We do not conclude, however, that we detect a third, low-mass planet within the current data.

Indeed, this 13.3-day period is near the stellar rotation period (~ 10 days, Sect. 3), so it could be at least partially caused by stellar rotation. However, no significant peaks are detected at this period (or at 30 days or 193 days) on the bisector periodograms. We interpret this 13.3-d signal as more likely due to aliases. To validate this, we constructed a fake radial velocity dataset with the same time sampling as our actual data, and that only includes the Keplerian model of the two planets found above. The periodogram of this fake dataset is almost identical to the one plotted in the upper panel Fig. 5: it of course includes the two peaks corresponding to the periods of the two planets, but also the peak at 13.3 days.

In addition to the one-day peak, the window function of our data shows a peak at ~ 14.3 days, indicating that this interval is favored in our time sampling. The 13.3-d signal could thus mainly come from the 14.3-day alias of the 192.9-day signal ($1/13.3 \approx 1/14.3 + 1/192.9$). In the second panel of Fig. 5 the periodogram of the residuals is plotted after subtraction of a fit including only the 30-day-period planet. The peak at 193 days is visible, as are these aliases at 1, 13.3, and 15.4 days

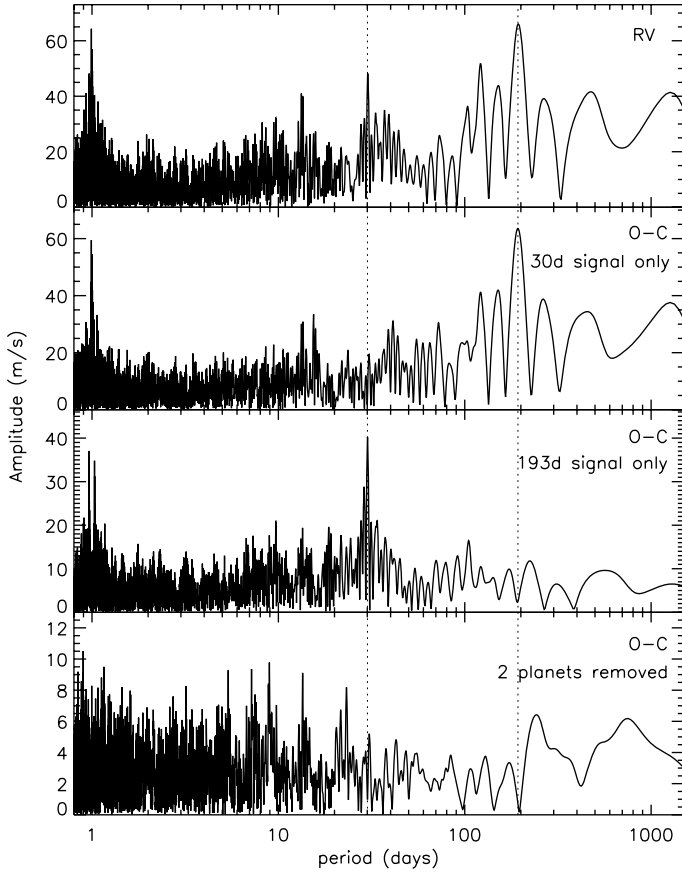


Fig. 5. Lomb-Scargle periodograms of the *SOPHIE* radial velocities. The *upper panel* shows the periodogram computed on the initial radial velocities, without any fit removed. The *second and third panels* show the periodograms computed on the residuals of the fits only including HD 9446b or HD 9446c, respectively. The *bottom panel* shows the periodogram after the subtraction of the 2-planet fit. The two vertical dotted lines show the periods of the two planets.

($1/15.4 \approx 1/14.3 - 1/192.9$). In the same manner, the third panel of Fig. 5 shows the periodogram of the residuals after a fit including only the 193-day-period planet. The peak at 193 days is no longer visible, and neither are the three aliases seen on the upper panel. This time the peak at 30 days is visible, together with these two aliases due to the 1-day favored sampling, at 0.97 and 1.03 day. The bottom panel of Fig. 5 shows the periodogram of the residuals after subtraction of the Keplerian fit including HD 9446b and HD 9446c. There are no remaining strong peaks on this periodogram; even the 1-day alias disappeared, showing that most of the periodic signals have been removed from the data. The remaining peaks are below 10 m/s amplitude, showing that the main part of the detected periodical signals in our data are caused by the two planets. The remaining signal in the residuals are at the limit of detection according to our accuracy. As in addition the stellar rotation period is close to an alias of the signal of HD 9446c, this makes difficult to characterize the radial-velocity signal due to stellar activity, which is mainly expected at the stellar rotation period. As the stellar jitter on the radial velocities is around 10 m s^{-1} , this effect on the derived parameters of the two detected planets is negligible.

The residuals of the measurements secured during the second observational season tend to be negative (Fig. 2, lower panel). This may suggest a possible additional component, with an orbital period close to or larger than the time span of our dataset

(2.3 years). Such an additional planet could not be established with the available data. For a ~ 2 -yr period, the projected mass of such a hypothetical planet should be lower than one Jupiter mass. On the other hand, over short periods, a hot-Jupiter is excluded in this system, since our dataset was accurate enough to detect it if there were any. The data allow planets with masses higher than $0.3 M_{\text{Jup}}$ and orbital periods shorter than 10 days to be excluded in the HD 9446 system.

5. Discussion

The data we have presented allow us to conclude that there is a planetary system around HD 9446, with at least two Jupiter-like planets, on 30 and 193-day orbits. HD 9446b has a slightly lower projected mass than Jupiter's mass; it is on a 0.2-eccentricity orbit, showing that tidal effects were not strong enough to circularize it. HD 9446c is at least 1.8 times more massive than Jupiter and is on a nearly-circular orbit. The host star of this system is slightly more metallic than the Sun, in agreement with the tendency found for stars harboring Jupiter-mass planets (see, e.g., Santos et al. 2005).

The mutual gravitational interactions between HD 9446b and HD 9446c are weak. The inner planet is stabilized on its orbit by the strong gravity of the star. Following Correia et al. (2005), a simulation of the two orbits from the current solution was run for 10^6 years, in order to estimate their evolution from mutual interactions. This shows no significant changes in the eccentricities, which remain in the ranges [0.18–0.23] and [0.03–0.075] for HD 9446b and HD 9446c, respectively. Therefore this system is stable for 10^6 years, and it also seems to be stable for longer time scales. We estimated the order of magnitude of the potential transit timing variations due to those weak mutual interactions, if any of the planets of the system does transit. For that purpose we performed another 3-body simulation of the system, assuming the masses of the planets are equal to the minimum masses and that the orbits are coplanar. We employed the Burlisch-Stoer algorithm implemented in the Mercury6 package (Chambers 1999) and integrated the system for 2000 days – i.e. around 10 orbits of the exterior planet. We found that the interaction between the planets produces variations in the central time of transits with small amplitude, which does not exceed 0.4 s for any of the two bodies.

No photometric search for transits has been managed for HD 9446. Depending on the unknown inclination i of the orbit, the transit probability for HD 9446b and HD 9446c are about 2% and 1%, respectively. There are more than 200 exoplanets detected from radial velocity surveys with orbital periods longer than 50 days, so with transit probabilities on the level of the percent. Only one is known to transit, namely HD 80606b (Moutou et al. 2009). It is likely that at least one or two more of these known long-period exoplanets are actually transiting, as seen from the Earth. Their search is challenging, because the times of the possible transits are not known accurately, especially a few years after the securement of the radial velocity data.

Among the more than 400 exoplanets discovered so far, almost 25% are located in the ~ 40 known multiple-planet systems. Most of them have been detected from radial velocity measurements. Additional planetary companions around HD 9446 cannot be detected with the available data besides the two planets reported, but they are of course possible, as multiple planet systems are common. For example HD 155358 (Cochran et al. 2007) has a Jupiter-mass planet on an orbit similar to HD 9446c, and another planet with a 530-day orbital period, or HD 69830 (Lovis et al. 2006) have two Neptune-mass planets on

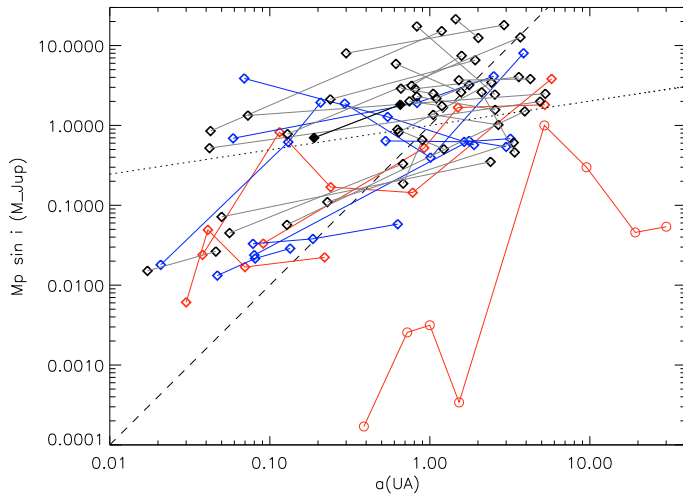


Fig. 6. Semi-major axes as a function of the projected masses for planets in multiple planet systems. 38 known extrasolar systems are plotted, with the planets of a given system that are linked by a solid line. The HD 9446-system is shown with filled diamonds. The fitted relation is plotted with a dotted line (mass proportional to $a^{0.3}$); the dashed line shows the a^2 relation. The 8 planets of the Solar System are also plotted for comparison (circles). Systems with two, three, and more planets are in black, blue, and red, respectively.

orbits similar to those of the two detected planets of HD 9446, and a third one on a 8.7-day orbit. More data are needed, and the monitoring of HD 9446 should thus be maintained. As low-mass planets tend to be found in multiple planetary systems (see, e.g., McArthur et al. 2004; Pepe et al. 2007; Mayor et al. 2009), HD 9446 should be considered for high-precision radial-velocity programs, despite its activity level.

The HD 9446 system presents a hierarchical disposition with the inner planet the less massive one and the outer planet more massive. Figure 6 displays the mass – semi-major axis relation for known multiple planetary systems. The data are taken from the compilation of the Extrasolar Planets Encyclopedia¹. Most of the known multiple planetary systems show this hierarchical disposition, roughly like the Solar System. The fitted relation between those two parameters provides a planet mass proportional to $a^{0.3}$ ($\propto a^{1.5}$ for the Solar System). The plot suggests the slope could be deeper for systems including low-mass planets. A positive slope could come from the higher migration efficiency for low-mass planets and/or to the fact that giant planets are preferentially formed at greater distances of their host stars than low-mass planets. However, observational biases are important here, as low-mass planets are easier to detect at short orbital periods from radial velocity variations. The semi-amplitude of the reflex motion of a star due to a planetary companion is proportional to $\sqrt{a} \times M_p \sin i$, so one could expect a a^2 -dependence in Fig. 6. As the averaged slope is lower, this could suggest that there is actually no strong dependence on average between those two parameters for multiple planet systems.

Figure 6 also shows that only a few multiple planetary systems include close-in giant planets. This agrees with Wright et al. (2009), who reported that single planet systems show a pileup at 3-day period and a jump at $a \approx 1$ AU, while

multiple planet systems show a more uniform distribution. Still, the close-in planets in systems with more than one planet are mainly low-mass planets. Hot Jupiters appear to be sparse in multiple planet systems, showing here again a distribution which is different from single planet systems. Only five hot-Jupiters are known to be in multiple planetary systems, namely HIP 14810b, ups And b, HAT-P-13b, HD 187123b, and HD 217107b. Single and multiple planet systems thus appear to have significant differences in some of their properties. Such differences may lead to a better understanding of the formation and evolution of those systems. Improving the statistics of extrasolar planets should be continued, in particular in multiple planet systems and with radial velocity surveys.

Acknowledgements. We thank A. C. M. Correia for help and discussions, as well as all the staff of Haute-Provence Observatory for their support at the 1.93-m telescope and on *SOPHIE*. We thank the “Programme National de Planétologie” (PNP) of CNRS/INSU, the Swiss National Science Foundation, and the French National Research Agency (ANR-08-JCJC-0102-01 and ANR-NT05-4-44463) for their support with our planet-search programs. D.E. is supported by CNES. N.C.S. would like to thank the support by the European Research Council/European Community under the FP7 through a Starting Grant, as well as from Fundação para a Ciência e a Tecnologia (FCT), Portugal, through a Ciência 2007 contract funded by FCT/MCTES (Portugal) and POPH/FSE (EC) and in the form of grants reference PTDC/CTE-AST/098528/2008 and PTDC/CTE-AST/098604/2008 from FCT/MCTES.

References

- Baranne, A., Queloz, D., Mayor, M., et al. 1994, *A&AS*, 119, 373
 Boisse, I., Moutou, C., Vidal-Madjar, A., et al. 2009a, *A&A*, 495, 959
 Boisse, I., Bouchy, F., Chazelas, B., et al. 2009b, New technologies for probing the diversity of brown dwarfs and exoplanets, EPJ Web of Conferences, in press [arXiv:1001.0794]
 Bouchy, F., Pont, F., Melo, C., et al. 2005, *A&A*, 431, 1105
 Bouchy, F., Hébrard, G., Udry, S., et al. 2009, *A&A*, 505, 853
 Chambers, J. E. 1999, *MNRAS*, 304, 793
 Cochran, W. D., Endl, M., Wittenmyer, R. A., & Bean, J. L. 2007, *ApJ*, 665, 1407
 Correia, A. C. M., Udry, S., Mayor, M., et al. 2005, *A&A*, 440, 751
 Da Silva, R., Udry, S., Bouchy, F., et al. 2008, *A&A*, 473, 323
 Fernandes, J., & Santos, N. C. 2004, *A&A*, 427, 607
 Hébrard, G., Bouchy, F., Pont, F., et al. 2008, *A&A*, 481, 52
 Hébrard, G., Udry, S., Lo Curto, G., et al. 2010, *A&A*, 512, A46
 Loeillet, B., Shporer, A., Bouchy, F., et al. 2008, *A&A*, 481, 529
 Lovis, C., Mayor, M., Pepe, F., et al. 2006, *Nature*, 441, 305
 McArthur, B., Endl, M., Cochran, W., et al. 2004, *ApJ*, 614, L81
 Mamajek, E. E., & Hillenbrand, L. A. 2008, *ApJ*, 687, 1264
 Mayor, M., Udry, S., Lovis, C., et al. 2009, *A&A*, 493, 639
 Melo, C., Santos, N. C., Gieren, W., et al. 2007, *A&A*, 467, 721
 Moutou, C., Hébrard, G., Bouchy, F., et al. 2009, *A&A*, 498, L5
 Noyes, R. W., Hartmann, L. W., Baliunas, S. L., Duncan, D. K., & Vaughan, A. H. 1984, *ApJ*, 279, 763
 Pepe, F., Mayor, M., Galland, F., et al. 2002, *A&A*, 388, 632
 Pepe, F., Correia, A. C. M., Mayor, M., et al. 2007, *A&A*, 462, 776
 Perruchot, S., Kohler, D., Bouchy, F., et al. 2008, in *Ground-based and Airborne Instrumentation for Astronomy II*, ed. McLean, I. S., Casali, M. M., Proc. SPIE, 7014, 70140J
 Perryman, M. A. C., Lindegren, L., Kovalevsky, J., et al. 1997, *A&A*, 323, L49
 Pont, F., Hébrard, G., Irwin, J. M., et al. 2009, *A&A*, 509, 695
 Queloz, D., Henry, G. W., Sivan, J. P., et al. 2001, *A&A*, 379, 279
 Santos, N. C., Mayor, M., Naef, D., et al. 2000, *A&A*, 361, 265
 Santos, N. C., Mayor, M., Naef, D., et al. 2002, *A&A*, 392, 215
 Santos, N. C., Israelian, G., & Mayor, M. 2004, *A&A*, 415, 1153
 Santos, N. C., Israelian, G., Mayor, M., et al. 2005, *A&A*, 437, 1127
 Santos, N. C., Udry, S., Bouchy, F., et al. 2008, *A&A*, 487, 369
 Wright, J. T., Upadhyay, S., Marcy, G. W., et al. 2009, *ApJ*, 693, 1084

¹ <http://exoplanet.eu>